Int J Adv Manuf Technol (2014) 71:81–90
DOI 10.1007/s00170-013-5480-1

ORIGINAL ARTICLE

Effect of tool pin profile on friction stir butt welding of high-zinc brass (CuZn40)

Afshin Emamikhah · Alireza Abbasi · Ali Atefat · M. K. Besharati Givi

Received: 26 September 2012 / Accepted: 5 November 2013 / Published online: 20 November 2013
© Springer-Verlag London 2013

Abstract In this experimental study, the effects of tool pin profiles (chamfered taper, single-threaded taper, three-flute, threaded cylinder, threaded taper, spline, and hexahedron) in friction stir welding of high-zinc brasses were explored through mechanical and micro-structural examinations. To evaluate the effect of temperature in friction stir welding, the temperature was measured by embedding thermo-couples within the fixture body. Furthermore, in order to evaluate the effects of the tool shape, the main FSW parameters (rotational speed, travel speed and plunge force) were maintained constant. Mechanical tests (hardness, tensile and bending) and micro-structural examinations were performed to study the properties of welded samples with regard to temperature measurement. The results indicated that suitable tools can generate enough heat below the shoulder due to further materials stirring. Moreover, studies of a hexahedron sample revealed that accumulated defects near the weld were one reason for mechanical weakening with regard to a lower heat generated.

Keywords Friction stir welding · High-zinc brass · Tool pin profile · Temperature measurement · Mechanical properties · Microstructure

A. Emamikhah (✉) · A. Abbasi · A. Atefat
Department of Mechanical Engineering, Najafabad Branch, Islamic Azad University, Technical Building # 1, P. O. Box: 8514143131, Isfahan, Iran
e-mail: A_emamikhah@azad.ac.ir

M. K. B. Givi
School of Mechanical Engineering, University College of Engineering, University of Tehran, Tehran, Iran

1 Introduction

Friction stir welding (FSW) has proven its advantages since 1991 when it was invented by Thomas et al. at The Welding Institute (TWI) basically for welding aluminium and its alloys [1]. Nowadays, this technique is used for welding the largest elements of space shuttles, panels of large ships, rocket fuel tanks and nuclear canisters. Welding of varied metals akin to steel, copper, titanium, aluminium and manganese of different sizes ranging from 0.5 to 50 mm in thickness and of varied joint designs such as butt, corner, lap, spot, T-shape, fillet and flexibility in joining pursuant to the advent of robotic techniques have distinguished this process. Figure 1 provides a comprehensive view of the terminology used in FSW.

According to Fig. 1, a non-consumable tool penetrates the abutting surfaces and dwells at the weld line. After dwell time, the movement of the tool becomes easier through the weld line (the boundary that has been formed by two plates) which consists of the advancing side (the half-plate that has the same direction as of the tool rotation and therefore the tool carries the material from it to another plate) and the retreating side and eventually a strong joint is created. Soundness of FSW joints directly depends on the main parameters which are engaged in the welding. Rotational speed, travel speed, plunge force and tool design are prominent parameters. The tool design is so important because it can help to more efficiently mixing the plasticized material [2–4]. Thus, the various forms of the pin and shoulder will have significant effects on the joints quality.

Brasses are alloys of copper distinct for their good strength and outstanding resistance to corrosion. Furthermore, apart from its appealing colour, electrical and thermal conductivity and fatigue resistance, formability of brass has led to its vast application in miscellaneous industries [5]. For these reasons, production of high-quality joints and use of the right method for welding seem absolutely necessary.

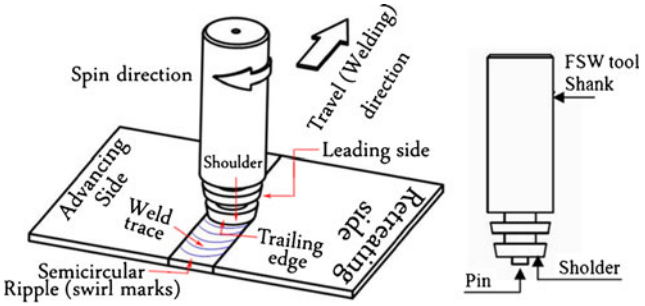

Fig. 1 Principle of the FSW process for butt joints

Muntz brass (CuZn40) or duplex brass usually contain between 38 and 42 % zinc. They are excellent for hot formability and forgeability for blanking, forming, bending, pressing, hot heading, upsetting and shearing. Hence, their applications include pipe fitting, domestic taps, radiator valves, gas appliances, window and door furniture, architectural panel sheets, large nuts and bolts, condenser plates and heat exchangers. The high quantity of zinc in brass has given it a dual phase structure, i.e. alpha-beta brasses. Alpha-beta brasses have higher hardness, strength, and entirely better mechanical properties. Also brasses of higher zinc contents have a lower cost and thus influence the total life-time costs [5].

Welding of Muntz brasses is so difficult because zinc diminishes the weldability of brass depending on its proportion [6]. Zinc has a low boiling temperature resulting in quick evaporation of zinc during welding and will finally leave a comparatively porous and weak layer of copper and copper oxide.

Another reason for inflexibility during the welding of brass is its high thermal diffusivity, which is about 10–100 times higher than that of steels and nickel alloys [6]. Also, since the thermal expansion coefficient of brass is greater than that of steel, a suitable fixture design is definitely needed to prevent distortion and separation of the plates. Although fusion-welding methods such as gas tungsten arc welding, gas metal arc welding and submerged arc welding have shown some success in welding low-zinc brasses, only shielded metal arc welding has hardly been recommended for welding high-zinc brasses with preheated to about 260–370 °C [6].

Concerning the problems occurring during fusion welding of brass, FSW has considerably decreased the defects and toxic vapours of zinc evaporation. Meran reported on the advantages of FSW over fusion welding methods for their zero evaporation and colour change during the welding of brass. Also, experimental studies established that the mechanical properties of brass (CuZn30) could be improved by controlling the principal parameters, i.e. rotational speed, travel speed and tool geometry [7].

Moghaddam et al. investigated the effect of travel speed on the FSW of brass plates (CuZn30) [8]. They showed that there is an accurate relationship between travel speed and a unique deformation pattern, namely “stir band”, in stir zone whose band density increases with the travel speed. Esmaeili et al. focused on the dissimilar joining of CuZn30 to aluminium 1050. They showed the ability of FSW in their study and suggested optimal parameters. Furthermore, they indicated that better joints are created owing to higher material flow and metallurgical bonding caused by more stirring and formation of onion rings [9].

In this research, for the first time, the effect of tool pin profiles on the formation of friction stir welding of high-zinc brasses (Muntz brass) was thoroughly investigated. Tensile, hardness, and bending tests were conducted to determine the mechanical properties of the weld. Also to evaluate the microstructure of the welds and elemental analysis, optical microscopy, scanning electron microscopy (SEM) and energy dispersive spectroscopy (EDS) were conducted for the defective samples. Moreover, to investigate the effect of temperature on the mechanical and microstructural properties, the temperature was precisely measured during welding. Mechanical and microstructural studies showed the important role of tool pin profile during FSW of brass (CuZn40).

Table 2 Mechanical properties of CuZn40

Material	Yield strength (Mpa)	Ultimate tensile strength (Mpa)	Elongation (%)	Young modulus (Gpa)	Poisson’ Ratio
CuZn40	133	300	52	105	0.34

2 Experimental procedure

The experiments were conducted on high-zinc brasses with dimensions of 100×70×3 mm. The chemical and mechanical properties of this metal are represented in Tables 1 and 2, respectively.

The plates were clamped in a butt-joint configuration using a fixture. The main reason for tightening the brass plates was the high thermal expansion coefficient and the very high pressures and forces occurring during FSW. In this study, a fixture was designed to achieve two goals as follows: (1)

Table 1 Chemical composition of CuZn40 (mass %)

Material	Sn	Pb	P	Mn	Fe	Ni	Si	Mg	Al	Co	Bi	Zn	Cu
CuZn40	0.005	0.0855	0.003	0.0032	0.134	0.005	0.005	0.005	0.002	0.013	0.0252	41.3	58.3

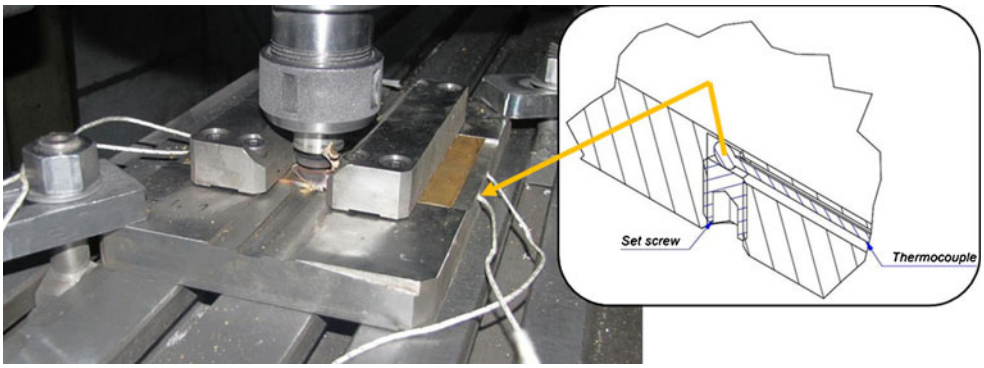

Fig. 2 Embedding thermocouples within the designed fixture body

clamp the brass plates against unwanted forces which result in pulling out the plates, (2) create locations in the fixture body to insert thermocouples for temperature measurement. Figure 2 indicates how thermocouples were embedded within the fixture. Furthermore, the thermocouples were placed precisely on the weld line boundary (tool motion boundary) and their distances from the top surface of fixture were kept 0.5 mm. Finally, to prevent displacement of thermocouples, socket screws were used to fasten them from the bottom surface of the fixture. The distances of thermocouples # 1 and 3 were assumed 35 and 65 mm on the advancing side of the start point of the weld and the thermocouples # 2 and 4 were placed on the retreating side of the weld at 50 and 65-mm intervals, respectively. In addition, the welding time was set at 7 min for 100-mm length of welding (the length of brass plates) with regard to the welding parameters maintained constant. Hence, during the welding process, the thermometer indicated the temperature contours from the attached thermocouples and the related diagrams were monitored from the Data Acquisition System (DAQ).

Also for accurate tool travel across the weld line (offset, 0), the fixture was precisely set for the spindle of the machine with a dial gauge and the centre of the tool was accurately aligned with the boundary of the plates (weld line) using an edge finder prior to welding.

In view of the fact that alternations in tool design can affect the uniformity of the weld, introducing more suitable tools will result in better mechanical properties and reduction in asymmetry [10, 11]. For these reasons, seven various tool pin profiles were fabricated from alloy hot-worked steel, namely X40CrMoV5-1 (material # 1.2344). Figure 3 indicates applied tools for producing joints during FSW of brass. Also, the main dimensions of the tools are presented in Table 3. All of the tools were approximately hardened to 60 HRC and then ground to the final sizes.

At the initial stage, to weld the brass plates in the experiment, all of the tools were shoulder-grooved, but since the brass stuck into the grooves (Fig. 4) resulting in defects and decreased mechanical properties through stirring, the design of the tools was modified to a flat shoulder. On the other hand, creating a flat shoulder would be cost-effective in that it decreases the machining time and remarkably increases the stirring and friction for bonding materials.

Notwithstanding the fact that the tools employed were designed on the previous ones referred to by TWI and other researchers [12], in this study, two new tools namely spline and hexahedron were used additionally to create the joints.

Considering the fact that FSW exerts considerable forces on the machine, selection of a machine with regard to the materials needed, FSW parameters and total life-time costs are crucial [13]. Therefore, the FSW of the brass plates was accomplished using a robust converted milling machine with a sturdy structure which greatly abated the vibrations. The power of electromotor was 4.5 kW with the possibility of choosing different speeds thanks to a variable gearbox system.

To explore the effects of different tools, the main FSW parameters were assumed constant. Table 4 indicates the experimental parameters for FSW which used for all welding. On completion of welding, to probe the effect of tools, all of the specimens were cut using wire EDM in order to analyze the mechanical and metallurgical properties. Tensile testing was performed on the transverse weld orientation samples conforming to ASTM E8M standard at a constant speed of 10 mm/min [14]. Three specimens were removed from the selected welds for the tensile test of every tool used. Additionally, to clarify the precise effect of FSW on the strength of the welds and remove the accumulated defects in the crown (top surface of the weld) and root (bottom) sides, 0.15 mm of both sides were eliminated by machining.

The bending test was used to ascertain the flexibility of joining and drawing properties of FSW samples using three-point method on both root in and root out configuration. To study the microstructural evolution via optical microscopy, samples were polished wet with sandpapers of 250 to 2,500 mesh sizes, and then to remove the abrasions, diamond paste and alcohol were used simultaneously on the disc-burnishing machine. Etching followed using a solution of 100 mL H_2O, 10 gr $FeCl_3$, 40 gr HCl and 25 gr HNO_3 for 15–20 s. SEM and EDS was employed to study the distinct area of the defected sample. In addition, the hardness profile was measured on the cross-section of the welds by Vickers microhardness test under a load of 20 kg for a dwell time of 10 s.

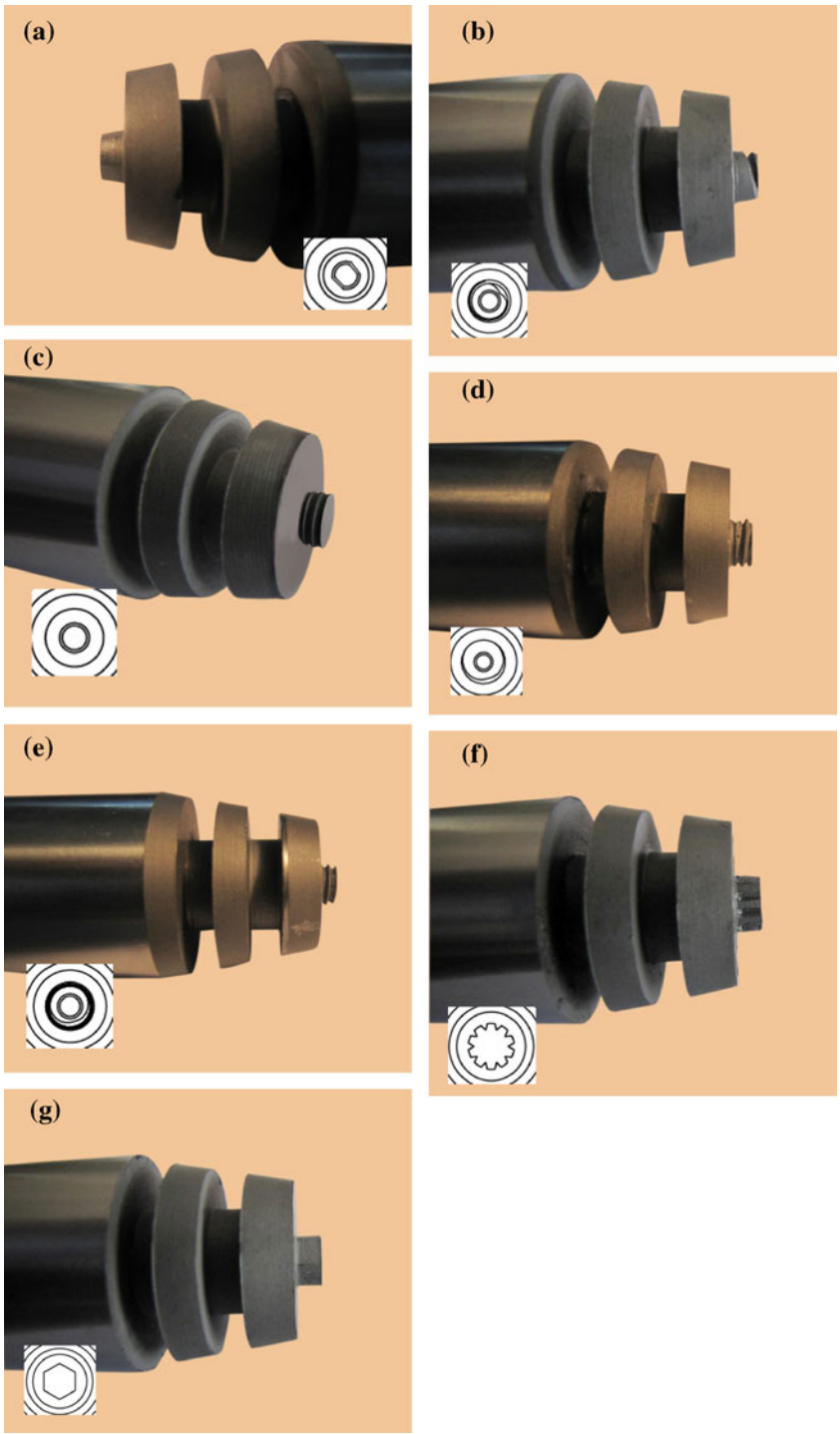

Fig. 3 Various tools used for welding brass plates: **a** chamfered taper, **b** single-threaded taper, **c** three- flute, **d** threaded cylinder, **e** threaded taper, **f** spline, **g** hexahedron

Table 3 Main FSW tool dimensions

Pin diameter	Shoulder diameter	Pin length	Tool length	FSW tool shank
6	18	2.8	80	25

3 Results and discussion

High zinc brasses were welded using different tools and predetermined welding parameters. For this purpose, first, appropriate tools were selected visually examining both sides of the joints. Obviously, production of improper tools apart from involving unsuitable parameters will result in FSW defects. In most cases, owing to proper penetration of the pins

Fig. 4 Brass sticking into shoulder grooves

correctly kept 0.05 mm away from the bottom surface of the plates, the defects appeared on the top rather than the bottom surfaces. Like a fabricated TWI tool namely Trivex, the chamfered taper tool revealed an entire crack after welding for want of stirring and mechanical work due to a smooth surface and blunt edges around the pin. Moreover, single-threaded taper tool showed an unacceptable appearance for disability to weld the brass plates and a three-flute tool did not complete the material bonding exposing a continuous groove such that it easily broke after welding. Figure 5 shows an FSW defect caused by single-threaded taper tool. Hence, subsequent investigations were naturally ignored for these welding samples. On the other hand, adequate welds by other tools, i.e. threaded cylinder, threaded taper, spline and hexahedron, were confirmed for next studies and were cited FSW1, FSW2, FSW3 and FSW4, respectively. The appearance of top and root surfaces of spline tool has been shown in Fig. 6.

3.1 Temperature measurement

A number of studies show that alterations in FSW major parameters will contribute to variations in the heat generated [15]. In 2008, Mandal et al. clearly stated that an increase in plunge force elevates the temperature and axial forces during friction stir spot welding of aluminium 2024 alloy [16]. In 2011, Moghaddam et al. indicated that during FSW of brass, temperature decreases with any increase in travel speed and this contributed to reduction in hardness [8].

However, in this study, to measure the temperature, the conditions are maintained equally throughout the welding stages. Since all of the major parameters were maintained constant (Table 4), temperature measurements relatively revealed the effect of tools on the heat generated during FSW. The extracted temperature diagrams are obtained following the welding. Figure 7 shows the temperature diagrams of FSW1, FSW2, FSW3, and FSW4 accordingly.

Table 4 Experimental parameters for FSW of brass

Rotational speed (RPM)	Travel speed (mm/min)	Tilt angle	Offset	Distance of pin from the bottom of plate (mm)
450	16	2.5	0	0.05

As for the temperature diagram of the threaded-cylinder tool, the temperature domains on both the advancing and retreating sides were nearly same. Also, the maximum heat generated by this tool was 501 °C on the advancing side and 453 °C on the retreating side. In fact, producing the thread on the cylinder caused the tool to properly mix the materials with its rotation. Thus, when the tool can easily mix the materials, it increases the stirring and temperature. On the contrary, as a result of induced frictional forces, producing plain tools can produce a lower temperature.

The maximum heat generated by a threaded taper tool was about 390 °C on the retreating side.

As shown for a spline tool, the discrepancy between the locations of thermocouples #1 and 2 on advancing and retreating sides indicated a higher temperature of about 417 °C on the advancing side, but the locations of thermocouples #3 and 4 were exactly the same and the temperature was nearly 405 °C on both sides. In comparison with the spline tool, the maximum temperature produced by the hexahedron tool was about 360 °C on both sides.

Firstly, these results show that welding conditions maintained constant, variations in the tool shape will affect the heat generated and the mixing of the materials under thermo-mechanical conditions. Furthermore, mechanical and microstructural properties will be heavily affected by the heat generated.

3.2 Hardness

The heat generated due to frictional forces and material stirring will leave a considerable effect on hardness. In this study, the main FSW parameters are maintained constant and the effects of tool pin profile on micro-hardness distribution have been examined. Micro-hardness distribution of the tools used is displayed in Fig. 8 on the cross section of the samples.

As shown, the hardness has relatively increased inside the welding zone. As shown in Fig. 8, the threaded-cylinder tool (FSW1) generated additional hardness on the advancing side. With regard to the temperature domain of FSW1 in the previous section, the increase in hardness is also correlated to the temperature increase on the advancing side. Hence, this experimental study confirms the relationship between temperature and hardness. However, other tools approximately had an equivalent hardness range except for the threaded taper tool (FSW2) that showed a small increase on the retreating side which was interestingly correlated to the temperature increase. Figure 9 shows the maximum hardness for different tool pin profiles and also for the base metal. As seen, the highest

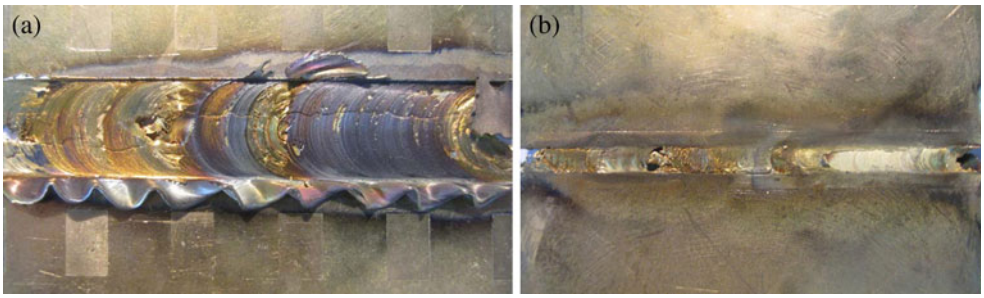

Fig. 5 Visual defects produced by single-threaded taper tool **a** top surface **b** weld root

hardness in the base metal is lower than the welded materials. This shows that thermo-mechanical conditions during the FSW of brasses have increased the overall hardness.

3.3 Tensile properties

The tensile properties of welded samples were determined to acquire the fracture locations and mechanical characteristics produced by different tool pin profiles. The results of stress–strain curves are compared in Fig. 10.

In comparison with the welded samples, the elongation of the base metal exceeded that of the welded samples. On the other hand, fracture locations of all welded samples occur in the base metal, with the exception of the hexahedron sample (FSW4) that fractured in the welding zone. The FSW4 sample also showed lower mechanical strength on bending test. To evaluate the weakness, microstructural studies were performed on the sample. Studies additionally indicated no dezincification in the welding area, but it proved as lack of materials bonding and accumulated defects on the top surface of the weld due to an unsuitable tool pin profile. Furthermore, referring to the temperature diagram of the hexahedron sample (FSW4), it indicates that the peak temperature of this sample is lower than those of the other samples. Thus, insufficient temperature implies weakness of the tool for stirring the materials.

It is obvious that the mechanical properties of the welded samples will be affected by different tool pin profiles due to variations in temperature. As for the spline tool, both hardness and elongation relatively increased and fracture occurred in the base metal. Moreover, the results of threaded taper tool comparatively tallied with those of the spline tool. In addition, the threaded cylindrical tool showed a good correlation between the hardness and tensile strength, but a slight reduction in ductility.

3.4 Bending tests

Bending test was applied to welded samples in both root-in and root-out configurations to clarify the formability and drawing properties of FSW joints. In 2009, Moreira et al. discussed that bending tests are very sensitive to the defects near the top and root surfaces of the weld [17]. They also approximately predicted the joint bending behaviour using a finite element model in ABAQUS software indicating a good correlation between simulation and experimentation with the maximum load. The dimensions of the samples for this test were assumed 100×10×3 mm. In addition, to estimate the bending behaviour of the samples in root-in and root-out configurations, two sound samples were taken from the welds. The downward speed of the bending punch was set at 1 mm/min. The main purpose for performing the bending tests was to evaluate the strength and bending behaviour of the welded samples. The samples were properly bent when the root-in method was used, but the hexahedron sample fractured under the load of 1.40 KN in the root-out method. Figure 11 compares the bending results for the spline (FSW3) and hexahedron (FSW4) samples.

As mentioned earlier in Section 3.3, it can probably be inferred that the hexahedron tool has lowered the temperature and materials bonding in the shoulder. In addition, microscopic studies showed considerable defects near the top surface of the weld which can be introduced as the major factors to increase the bending fracture.

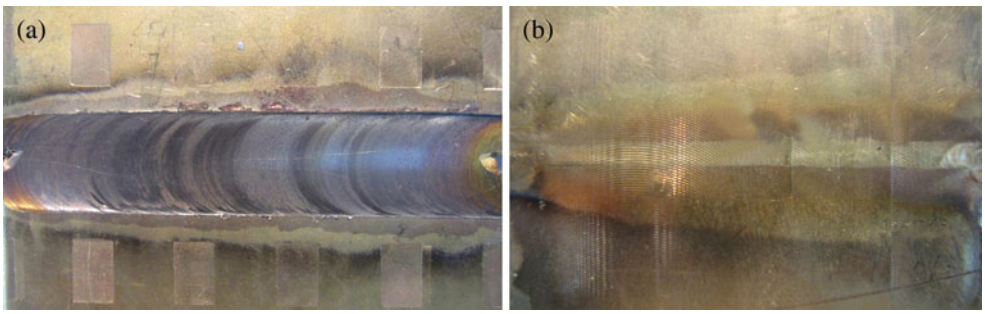

Fig. 6 Effect of spline tool (FSW3) on the top (**a**) and root (**b**) surfaces of the weld

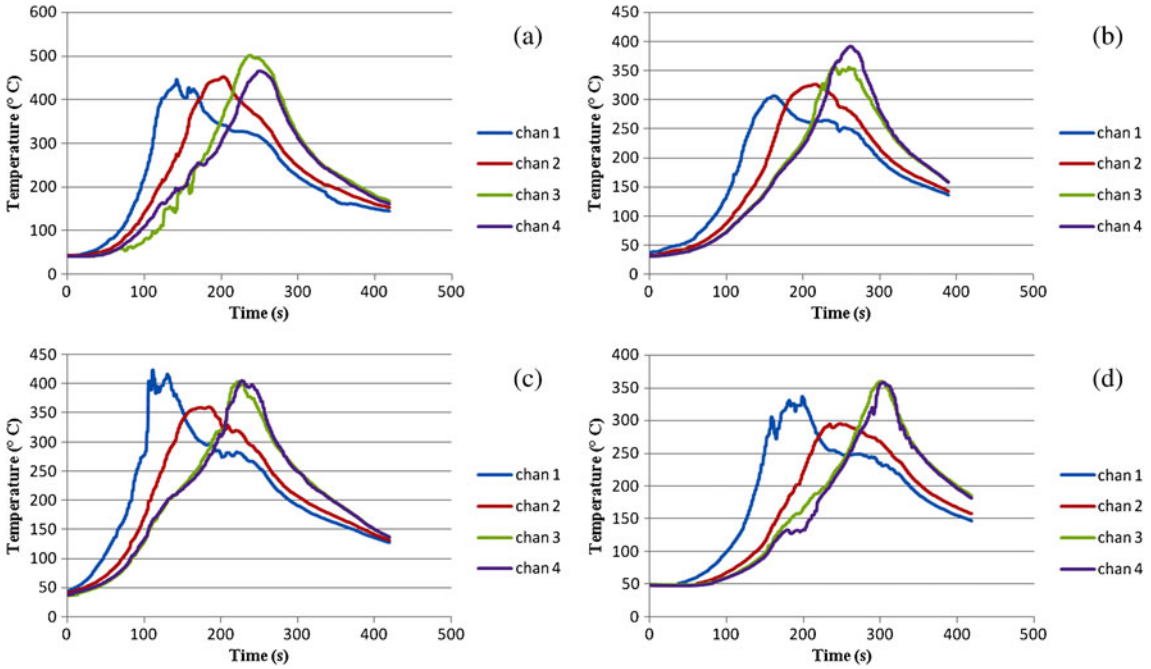

Fig. 7 The temperature diagrams extracted after 7 min: **a** threaded cylinder (FSW1), **b** threaded taper (FSW2), **c** spline (FSW3), **d** hexahedron (FSW4)

3.5 Microstructural examinations

Materials stirring below the tool during the FSW exposes the microstructural regions, i.e. stir zone or nugget, the thermo-mechanically-affected zone (TMAZ), heat-affected zone and the base metal which will be generated correspondingly from the weld centre to the outward parts [18]. The microstructural evolution of the welded samples was investigated to find a correlation between temperature measurement and mechanical studies as well as fracture occurrence in the hexahedron sample (FSW4). As shown in Fig. 12, optical microscopy showed that grain sizes were remarkably altered from the base metal to the stir zone.

In fact, mechanical work as an effect of the tool rotation and stirring action below the shoulder will transmute the dominant grains to finer ones. Additionally, the heat generated during welding helps improve the material bonding and grain refining. Hence, the thermo-mechanical conditions

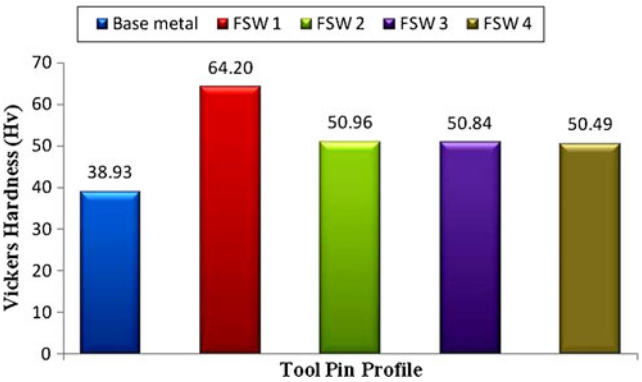

Fig. 9 Maximum hardness of the samples compared to that of the base metal

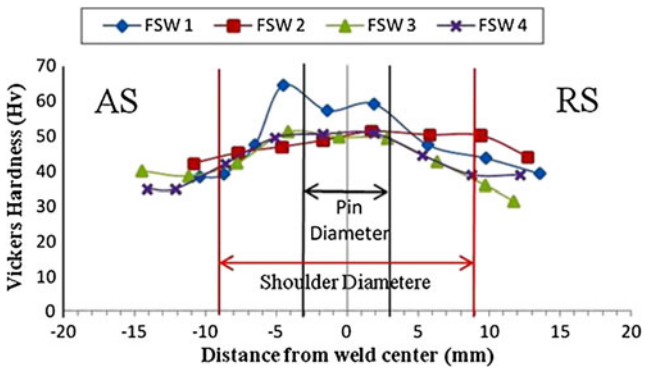

Fig. 8 Micro-hardness distributions of selected samples on the cross section of the welds

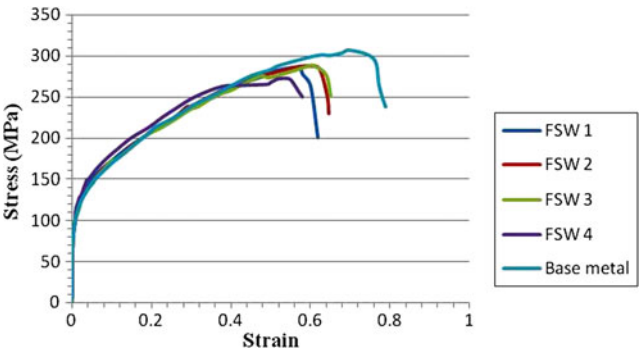

Fig. 10 Effects of friction stir welding on stress–strain curves

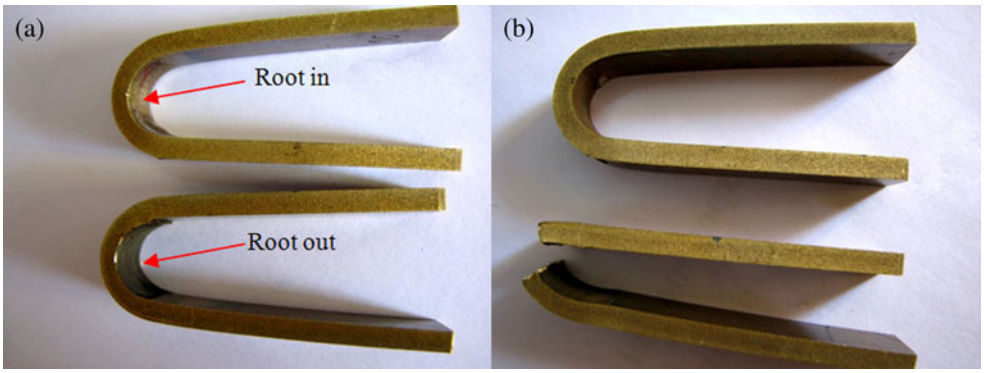

Fig. 11 Effects of bending test on root-in and root-out methods: **a** spline, **b** hexahedron

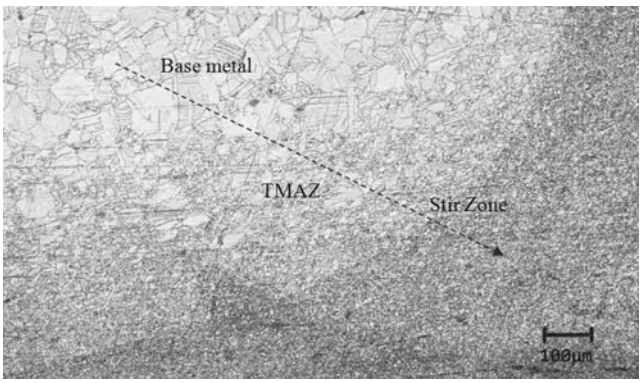

Fig. 12 Effect of FSW on microstructural evolution from the base metal to the stir zone

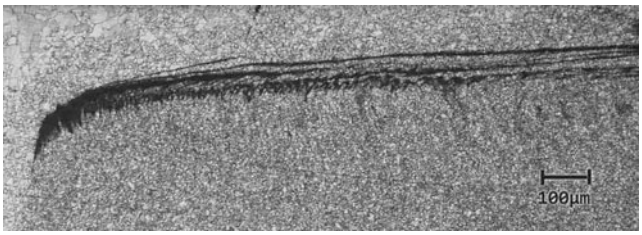

Fig. 14 Apparent defects caused by a hexahedron tool

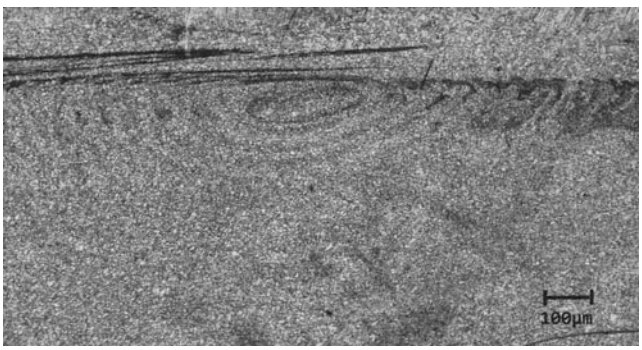

Fig. 13 Formation of onion rings on the top part of the stir zone using a hexahedron tool

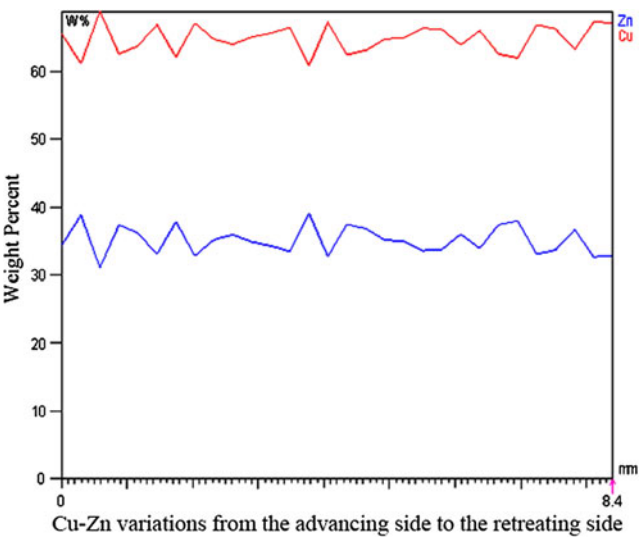

Fig. 15 The Cu-Zn variations from the advancing side to the retreating side

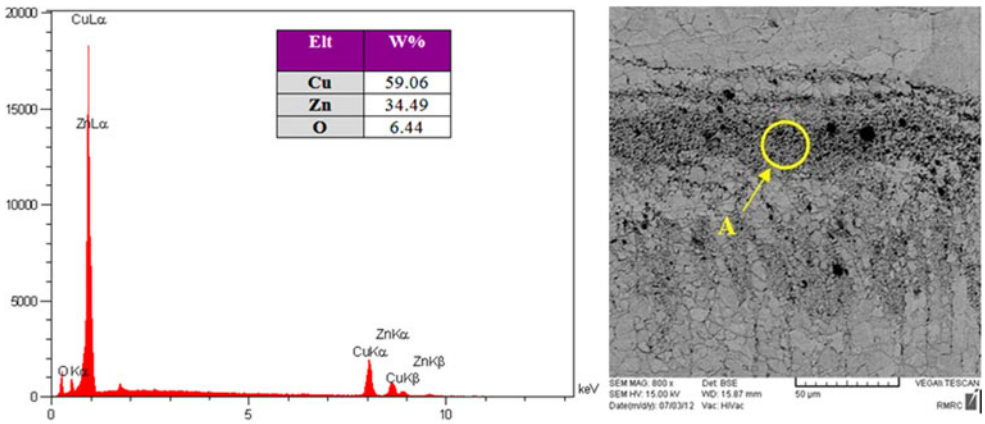

Fig. 16 SEM and EDS analyses from the stir zone

below the shoulder and around the pin will leave decisive effects on the mechanical and microstructural properties of the brass plates.

A well-defined region, i.e. TMAZ, affected by the inherent characteristics of the FSW was clearly noted between the stir zone and base metal (Fig. 12). High-zinc brass comprises two phases: one prevailing between the sample area and β phase that increases the hardness and hot-formability of brass [5]. According to the grain refining in Fig. 12, continuous rotation of the pin and materials stirring properly broke down the α+β phase into small particles within the stir zone. A unique lamellar and vortex-like pattern namely onion rings was seen in FSW4 according to Fig. 13.

The essential reason for formation of this pattern is material rotation beneath the shoulder. In the event of FSW4, mechanical investigations showed low properties due to accumulated defects on the top surface of the weld (Sections 3.3 and 3.4). These accumulated defects are shown in Fig. 14 that seems to be the result of the materials sticking to the tool and burning due to induced frictional forces.

To find out why the hexahedron sample fractured on the mechanical test plus to accumulated defects, a chemical analysis of copper and zinc was also performed through 30 points on a line from the advancing side to the retreating side. As shown in Fig. 15, the Cu-Zn variations were not so vast.

In addition, SEM and EDS from the stir zone showed no dezincification (Fig. 16).

With regard to microstructural studies on the hexahedron sample (FSW4), it was noted that the hexahedron tool did not generate heat sufficient for materials stirring resulting in formation of accumulated defects on the top surfaces of the weld. Apart from this, optical microscopy was used to check the possible defects in other samples. A uniform pattern without any defects was seen in the samples. Hence, a good weld can be produced if a suitable tool is used with the right process parameters.

4 Conclusions

In this research, the effects of tool pin profiles on friction stir welding of high zinc brasses were experimentally studied. The main conclusions are summarized as follows:

1. Friction stir welding of high zinc brasses (Muntz brasses) was properly performed using different tool pin profiles. In order to increase the material stirring and produce a heat below the shoulder, the grooves were eliminated from the shoulder surface. Also, to determine the effect of tool shape, the main FSW parameters were assumed constant and four tools, i.e. threaded cylinder, threaded taper, spline and hexahedron were selected for further investigations.
2. Temperature was measured during the welding by embedding the thermocouples within the designed fixture. The extracted data showed a lower temperature generated by the hexahedron tool than other tools due to the flat faces around the pin. On the other hand, the threaded-cylinder tool showed a higher heat generated, i.e. 501 °C generated on the advancing side. In fact, temperature measurement revealed that in a proper range of process parameters, suitable tools can properly increase the heat and helps improve material stirring below the shoulder.
3. Studies showed a relatively higher hardness of the welding zone than of the base metal due to grain refinement. Also, a close relationship was observed between the temperature and hardness, i.e. it resulted in a higher temperature and hardness (the higher the temperature, the higher the hardness). As for the threaded-cylinder tool, both hardness and temperature increased on the advancing side. Moreover, an increase in temperature and hardness was achieved by a threaded taper tool on the retreating side.
4. The results of the spline and threaded taper tool samples relatively tallied. Both the hardness and tensile strength increased using the FSW tools.

5. Tensile and bending tests revealed that the hexahedron sample had poorer mechanical properties due to fracture in the welding zone. Microstructural examinations on the hexahedron sample revealed that the accumulated defects near the top surface of the weld are one reason for mechanical weakening with regard to the lower temperature and mechanical work under the welding conditions.

References

1. Thomas WM, Nicholas ED, Needham JC, Murch MG, Templesmith P, Dawes CJ (1991) Friction stir butt welding, GB Patent No. 9125978.8, International patent application No. PCT/GB92/02203
2. Elangoven K, Balasubramanian V (2008) Influences of tool pin profile and welding speed on the formation of friction stir processing zone in AA2219 aluminium alloy. J Mater Process Tech 200:163–175
3. Nandan R, Debroy T, Bhadeshia HKDH (2008) Recent advances in friction stir welding-process, Weldment structure and properties. Prog Mater Sci 53:980–1023
4. Elangovan K, Balasubramanian V (2007) Influences of pin profile and rotational speed of the tool on the formation of friction stir processing zone in AA2219 aluminium alloy. Mater Sci Eng A 459:7–18
5. ASM (1990) Properties and selection: nonferrous alloys and special-purpose materials. ASM, Cleveland
6. ASM (1993) Welding, brazing, and soldering. ASM, Cleveland
7. Meran C (2006) The joints properties of brass plates by friction stir welding. Mater Design 27:719–726
8. Sarvghad Moghaddam M, Parvizi R, Haddad-Sabzevar M, Davoodi A (2011) Microstructural and mechanical properties of friction stir welded Cu-30Zn brass alloy at various feed speeds: influence of stir bands. Mater Design 32:2749–2755
9. Esmaeili A, Besharati Givi MK, Zareie Rajani HR (2011) A metallurgical and mechanical study on dissimilar friction stir welding of aluminium 1050 to brass (CuZn30). Mater Sci Eng A 528:7093–7102
10. Thomas WM, Johnson KI, Wiesner CS (2003) Friction stir welding-recent developments in tool and process technologies. Adv Eng Mater 5:485–490
11. Zhao YH, Lin SB, Qu F, Wu L (2006) Influence of pin geometry on material flow in friction stir welding process. J Mater Sci Technol 22:45–50
12. Aissani M, Gachi S, Boubenider F, Benkedda Y (2010) Design and optimization of friction stir welding tool. Mater Manuf Process 25:1199–1205
13. Bahemmat P, Haghpanahi M et al (2012) Study on dissimilar friction stir butt welding of AA7075-O and AA2024-T4 considering the manufacturing limitation. Int J Adv Manuf Technol 59:939–953
14. Standard test Method for Tension Testing of Metallic Materials (1998) ASTM E 8M Annual Book of ASTM Standards, Part 8, ASTM
15. Schmidt H, Hattel J (2005) Modelling heat flow around tool probe in friction stir welding. Sci Technol Weld Joi 10:176–186
16. Mandal S, Rice J, Elmustafa AA (2008) Experimental and numerical investigation of the plunge stage in friction stir welding. J Mater Process Tech 203:411–419
17. Moreira PMGP, Santos T et al (2009) Mechanical and metallurgical characterization of friction stir welding joints of AA6061-T6 with AA6082-T6. Mater Design 30:180–187
18. Saeid T, Abdollah-zadeh A, Shibayanagi T, Ikeuchi K, Assadi H (2010) On the formation of grain structure during friction stir welding of duplex stainless steel. Mater Sci Eng A 527:6484–6488